

Terahertz amplifiers based on gain reflectivity in cuprate superconductors

Guido Homann,¹ Jayson G. Cosme,² and Ludwig Mathey^{1,3}

¹Zentrum für Optische Quantentechnologien and Institut für Laserphysik, Universität Hamburg, 22761 Hamburg, Germany

²National Institute of Physics, University of the Philippines, Diliman, Quezon City 1101, Philippines

³The Hamburg Centre for Ultrafast Imaging, Luruper Chaussee 149, 22761 Hamburg, Germany

(Dated: September 7, 2021)

We demonstrate that parametric driving of suitable collective modes in cuprate superconductors results in a reflectivity $R > 1$ for frequencies in the low terahertz regime. We propose to exploit this effect for the amplification of coherent terahertz radiation in a laser-like fashion. As an example, we consider the optical driving of Josephson plasma oscillations in a monolayer cuprate at a frequency that is blue-detuned from the Higgs frequency. Analogously, terahertz radiation can be amplified in a bilayer cuprate by driving a phonon resonance at a frequency slightly higher than the upper Josephson plasma frequency. We show this by simulating a driven-dissipative $U(1)$ lattice gauge theory on a three-dimensional lattice, encoding a bilayer structure in the model parameters. We find a parametric amplification of terahertz radiation at zero and nonzero temperature.

Coherent radiation sources in the terahertz regime have applications in spectroscopy and imaging in numerous fields, such as biology and medical diagnostics, nondestructive evaluation, and solid state research [1–5]. While significant progress has been made in the development of powerful terahertz sources [6–12], further development of terahertz technologies is imperative to close the ‘terahertz gap’, particularly in the range between 0.5 and 1.5 THz [10, 11]. In this work, we propose the design of an optical parametric oscillator in the low-terahertz regime, i.e., ~ 1 THz, to be utilized as an optical amplifier in a laser-like operation. We base this design on a general strategy to control the reflectivity of solids. The central mechanism is to use a collective mode with a nonlinear coupling to the electromagnetic field for parametric amplification. We apply this mechanism to cuprate superconductors and propose a laser-like setup for the amplification of terahertz radiation. In this setup, a light-driven superconductor with reflectivity $R_2 = R(\omega_{\text{pr}}) > 1$ serves as one of three mirrors forming an optical resonator as depicted in Fig. 1. The probe with frequency ω_{pr} enters the resonator through a partially transparent mirror with reflectivity $R_1 < 1$ and transmissivity $T_1 > 0$. The third mirror is assumed to have perfect reflectivity $R_3 = 1$. For $R_1 R_2 < 1$, the intensity ratio of the outgoing and the ingoing signal is given by

$$\frac{I_{\text{out}}}{I_{\text{in}}} = \frac{R_2 T_1^2}{1 - R_1 R_2} + R_1. \quad (1)$$

The gain condition of this setup, $R_2 > 1/R_1$, is reflected by the divergence of I_{out} for $R_1 R_2 \rightarrow 1$. Above this threshold, the gain saturates once the probe signal enters the nonlinear response regime such that $R(\omega_{\text{pr}})$ decreases. With our proposal, we extend the scope of light control of cuprate superconductors to the amplification of terahertz radiation in an optical parametric oscillator [13–15]. We note that reflectivities $R > 1$ for light-driven solids were discussed in Refs. [16, 17].

We first demonstrate parametric amplification of ter-

ahertz radiation in monolayer cuprates using a gauge-invariant two-mode model with a cubic coupling process of the Higgs and plasma modes [18, 19]. We find that driving plasmonic excitations blue-detuned from the Higgs mode leads to a reflectivity $R > 1$ for probe frequencies below the Josephson plasma edge. As a second example, we consider a periodic modulation of the interlayer tunneling in bilayer cuprates, which models a periodic excitation of a phonon mode. Here, the low-frequency reflectivity is larger than 1 when the frequency of the excited phonon mode is blue-detuned from the upper Josephson plasma frequency. We implement a three-dimensional $U(1)$ lattice gauge theory with anisotropic lattice parameters to simulate this scenario at nonzero temperature. Our calculations show that phonon mediated amplification of terahertz radiation is effective at temperatures up to $\sim 20\%$ of the critical temperature T_c .

The key requirement for the proposed amplification mechanism is a cubic coupling term of the form $\phi\theta^2$ in the Lagrangian, where θ is the plasma mode and ϕ represents another collective mode. Note that the plasma mode directly couples to the electric field E . When one applies pump and probe processes to the system, as sketched in Fig. 2(a), there are two scenarios for a parametric amplification of the probe. In one scenario, the pump directly excites the plasma mode θ at a frequency that is blue-detuned from the eigenfrequency of the mode ϕ , which

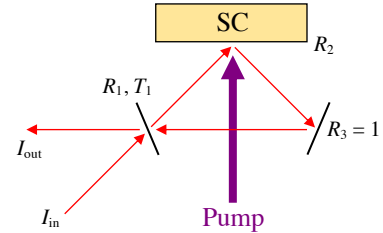


FIG. 1. Setup of an optical parametric oscillator using a superconductor (SC) with reflectivity $R_2 > 1$ as a gain medium.

acts as an idler mode. Alternatively, the pump primarily couples to the collective mode ϕ . An enhanced response is then achieved for a pump frequency ω_{dr} that is blue-detuned with respect to the plasma frequency. Here, the plasma mode serves as the idler mode. In both cases, the probe couples to the plasma mode, and its frequency should be $\omega_{\text{pr}} = \omega_{\text{dr}} - \omega_{\text{r}}$, where ω_{r} denotes the eigenfrequency of the idler mode. Thus, three-wave mixing of the probe with the pump and resonant excitations of the idler mode induces the amplification of the probe signal. An important signature of this effect is a negative peak in the real part of the optical conductivity σ_1 at $\omega_{\text{pr}} = \omega_{\text{dr}} - \omega_{\text{r}}$. A negative conductivity has also been predicted for light-driven graphene recently [20].

Josephson plasma oscillations are characteristic excitations of cuprate superconductors [21–25], corresponding to the tunneling of Cooper pairs between copper-oxide layers. The Higgs mode, on the other hand, describes amplitude oscillations of the superconducting order parameter [26–32]. While plasma modes directly couple to the electromagnetic vector potential, the Higgs mode has no linear coupling to electromagnetic fields in a system with approximate particle-hole symmetry [33, 34]. A two-mode model of a light-driven monolayer cuprate at zero temperature was derived in Refs. [18, 19]. The underlying Lagrangian includes a cubic term $\sim h\theta^2$, coupling the plasma mode θ and the Higgs mode h . The equations of motion read

$$\ddot{\theta} + \gamma_{\text{J}}\dot{\theta} + \omega_{\text{J}}^2 \sin(\theta)(1+h)^2 = j, \quad (2)$$

$$\begin{aligned} \ddot{h} + \gamma_{\text{H}}\dot{h} + \omega_{\text{H}}^2 \left(h + \frac{3}{2}h^2 + \frac{1}{2}h^3 \right) \\ + 2\alpha\omega_{\text{J}}^2 [1 - \cos(\theta)](1+h) = 0, \end{aligned} \quad (3)$$

where ω_{H} is the Higgs frequency, ω_{J} is the plasma frequency, and γ_{H} and γ_{J} are damping coefficients. The capacitive coupling constant α is of the order of 1 in cuprate superconductors [35]. The interlayer current $j(t) = j_{\text{dr}}(t) + j_{\text{pr}}(t)$ is induced by an external electric field polarized along the c axis of the crystal and describes the pump and probe processes. A monochromatic pump with field strength E_0 gives rise to $j_{\text{dr}}(t) = (-2ed\omega_{\text{dr}}E_0/\hbar\epsilon_{\text{r}})\sin(\omega_{\text{dr}}t)$, where $-2e$ is the Cooper pair charge, d is the interlayer spacing, and ϵ_{r} is the dielectric constant of the material. To calculate the optical conductivity, we include a weak probe current $j_{\text{pr}}(t)$ and evaluate the Fourier components $j(\omega_{\text{pr}})$ and $\theta(\omega_{\text{pr}})$ in the steady state. The conductivity is given by $\sigma(\omega) = ie_{\text{r}}\epsilon_0 j(\omega_{\text{pr}})/\omega_{\text{pr}}\theta(\omega_{\text{pr}})$, as follows from the Josephson relation $\dot{\theta} = 2edE/\hbar$ [36].

In Figs. 2(b) and 2(c), we present numerical results for the real part of the optical conductivity of a monolayer cuprate with Josephson plasma frequency $\omega_{\text{J}}/2\pi = 2$ THz and Higgs frequency $\omega_{\text{H}}/2\pi = 6$ THz. For a pump frequency that is red-detuned with respect to the Higgs frequency, σ_1 exhibits a pronounced absolute maximum

at $\omega_{\text{pr}} \approx \omega_{\text{H}} - \omega_{\text{dr}}$ and a local maximum at $\omega_{\text{pr}} \approx \omega_{\text{H}} + \omega_{\text{dr}}$. The peak at $\omega_{\text{pr}} \approx \omega_{\text{H}} - \omega_{\text{dr}}$ corresponds to an excitation of the Higgs mode via resonant two-photon processes, whereas a probe with $\omega_{\text{pr}} \approx \omega_{\text{H}} + \omega_{\text{dr}}$ amplifies the pump signal and simultaneously excites the Higgs mode. The small minimum slightly below 15 THz results from the coupling of the probe to the third-harmonic of the pump.

For a blue-detuned pump frequency, we find $\sigma_1 < 0$ for low probe frequencies. The minimum at $\omega_{\text{pr}} \approx \omega_{\text{dr}} - \omega_{\text{H}}$ indicates a resonant amplification of the probe due to a down-conversion of the pump by simultaneous excitation of the Higgs mode. The conductivity displays a maximum at $\omega_{\text{pr}} \approx \omega_{\text{dr}} + \omega_{\text{H}}$, similarly to the case of a red-detuned pump frequency, while the third-harmonic of the pump is outside the plotted frequency range. In the Sup-

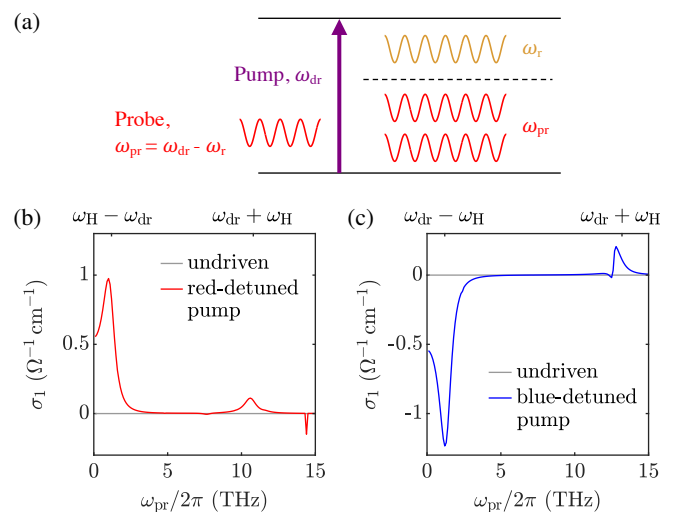


FIG. 2. Parametric amplification of terahertz radiation in a solid with a plasma mode θ and a collective mode ϕ that are nonlinearly coupled. (a) Schematic illustration of the amplification process. The pump laser excites the plasma mode θ (or the collective mode ϕ) with frequency ω_{dr} . The pump signal is down-converted to the lower frequency $\omega_{\text{pr}} = \omega_{\text{dr}} - \omega_{\text{H}}$ of the probe by simultaneous excitation of the collective mode ϕ (or the plasma mode θ) at its eigenfrequency ω_{r} . The numerical results in (b) and (c) are obtained for a monolayer cuprate, in which Josephson plasma oscillations are driven by the pump laser and the Higgs mode is the idler mode. (b) When the pump frequency is red-detuned from the Higgs frequency $\omega_{\text{r}} \equiv \omega_{\text{H}}$, a probe with $\omega_{\text{pr}} \approx \omega_{\text{H}} - \omega_{\text{dr}}$ is attenuated as indicated by the positive peak in the real part σ_1 of the optical conductivity. The pump frequency is $\omega_{\text{dr}}/2\pi = 4.8$ THz and the pump strength is $E_0 = 150$ kV/cm. (c) A blue-detuned pump frequency leads to an amplification of the probe for $\omega_{\text{pr}} \approx \omega_{\text{dr}} - \omega_{\text{H}}$, corresponding to a negative peak in σ_1 . In this case, the pump frequency is $\omega_{\text{dr}}/2\pi = 7.2$ THz and the pump strength is $E_0 = 300$ kV/cm. The probe strength is $E_{\text{pr}} = 1$ kV/cm in both cases. The Josephson plasma frequency is $\omega_{\text{J}}/2\pi = 2$ THz and the Higgs frequency is $\omega_{\text{H}}/2\pi = 6$ THz. The remaining parameters are $\gamma_{\text{J}}/2\pi = 0.5$ THz, $\gamma_{\text{H}}/2\pi = 1$ THz, $\alpha = 1$, $\epsilon_{\text{r}} = 4$, and $d = 10$ Å.

plemental Material, we provide an analytical estimate of $\sigma(\omega_{\text{pr}} = \omega_{\text{dr}} - \omega_{\text{H}})$ based on a perturbative expansion for weak pump-probe strengths [37]. Our analytical estimate is in qualitative agreement with the numerical results.

In the following, we focus on pump frequencies that are blue-detuned from the Higgs frequency. As we shall see below, a negative conductivity σ_1 implies a reflectivity $R > 1$ at low frequencies. The reflectivity at normal incidence is obtained from the optical conductivity via the Fresnel equation

$$R(\omega) = \left| \frac{1 - \sqrt{\epsilon(\omega)}}{1 + \sqrt{\epsilon(\omega)}} \right|^2, \quad (4)$$

with the complex permittivity $\epsilon(\omega) = \epsilon_r + i\sigma(\omega)/\epsilon_0\omega$. If the real part ϵ_1 of the permittivity is negative, we take its square root such that the imaginary part of the solution is positive. This corresponds to an exponential decay of the electric field from the surface into the bulk, which is the characteristic response of a Josephson plasma for frequencies below its plasma edge at $\omega_{\text{J}}/\sqrt{2}$.

Figure 3 displays the low-frequency reflectivity for different pump strengths and frequencies of the optical pump applied to the same monolayer cuprate as before. For moderate pump strengths, such as in Fig. 3(a), the reflectivity always spikes up just below the plasma edge, irrespective of the pump frequency. This is an immediate consequence of the negative σ_1 at low probe frequencies. The amplification mechanism is particularly effective if the detuning $\omega_{\text{dr}} - \omega_{\text{H}}$, and thus the minimum of σ_1 , approaches the plasma edge frequency, as is the case for $\omega_{\text{dr}}/2\pi = 7.2$ THz. The behavior notably changes for higher pump strengths as evidenced by Fig. 3(b). At these pump strengths, the plasma edge shifts to a lower frequency. The magnitude of the shift depends on the pump frequency, and the reflectivity becomes large for smaller detuning than $\omega_{\text{dr}} - \omega_{\text{H}}$. Both the maximal reflectivity and the frequency domain of enhanced reflectivity are comparable for the lowest pump frequency ($\omega_{\text{dr}}/2\pi = 6.6$ THz) and the pump frequency with nearly optimal detuning ($\omega_{\text{dr}}/2\pi = 7.2$ THz).

We now turn to our second example of parametric amplification of terahertz radiation in cuprate superconductors. While the Higgs mode is strongly damped in the cuprates in general [28, 29, 38], phononic excitations have picosecond lifetimes, such as vibrations of apical oxygen atoms in YBCO [39, 40]. Therefore, we consider the scenario in which the pump laser resonantly couples to a phonon mode.

Specifically, we consider bilayer cuprates utilizing a relativistic $U(1)$ lattice gauge theory in three dimensions [18, 19]. We formulate a Lagrangian with dynamical and static terms on an anisotropic lattice that corresponds to a bilayer structure as illustrated in Fig. 4(a). The static part of the Lagrangian resembles the Ginzburg-Landau free energy [41]. That is, we describe the Cooper pairs as

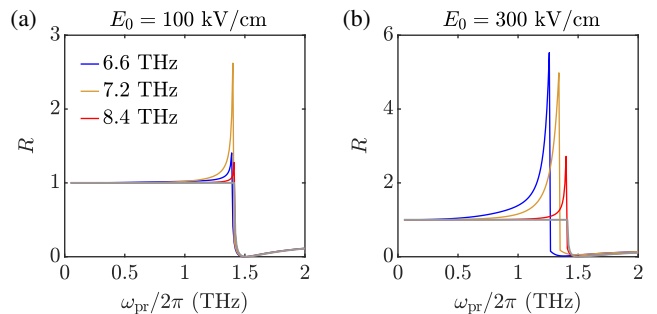


FIG. 3. Higgs mode mediated amplification of terahertz radiation in a monolayer cuprate. The reflectivity at normal incidence is shown for two choices of the pump strength: (a) $E_0 = 100$ kV/cm, (b) $E_0 = 300$ kV/cm. The pump frequencies for the higher pump strength in (b) are the same as indicated for the lower pump strength in (a). Gray lines correspond to the undriven case. The probe strength is $E_{\text{pr}} = 1$ kV/cm. The model parameters are the same as in Fig. 2.

a condensate of interacting bosons with charge $-2e$, represented by the complex field $\psi_{\mathbf{r}}$. This model is suitable for simulating the coupled dynamics of the order parameter of the superconducting state and the electromagnetic field at temperatures below T_c .

The order parameter $\psi_{\mathbf{r}}(t)$ is located on the lattice sites. According to the Peierls substitution, each component of the electromagnetic vector potential $A_{k,\mathbf{r}}(t)$ is defined on the bond between the site \mathbf{r} and its nearest neighbor in the $k \in \{x, y, z\}$ direction. The intra- and interbilayer spacings $d_{s,w}$ are taken as the distances between the CuO_2 planes in the crystal, and the in-plane discretization length d_{ab} is introduced as a short-range cutoff of the order of the in-plane coherence length. The bilayer structure results in the appearance of two Josephson plasma modes. The lower Josephson plasma resonance is dominated by interbilayer currents, due to the interlayer tunneling energy t_w . The upper Josephson plasma resonance, on the other hand, is dominated by intrabilayer currents, due to the intralayer tunneling energy t_s . We choose the tunneling coefficients t_s and t_w to yield realistic values for the Josephson plasma frequencies. The in-plane tunneling coefficient t_{ab} does not only define an in-plane plasma frequency but also sets the critical temperature of the system.

We add damping terms and Langevin noise to the equations of motion, which are given by the Euler-Lagrange equations. This enables us to numerically determine the time evolution of the order parameter and the vector potential at zero and nonzero temperature. We employ periodic boundary conditions and integrate the stochastic differential equations using Heun's method with a step size of $\Delta t = 1.6$ as. To mimic the effect of a driven phonon mode, we make the interlayer tunneling

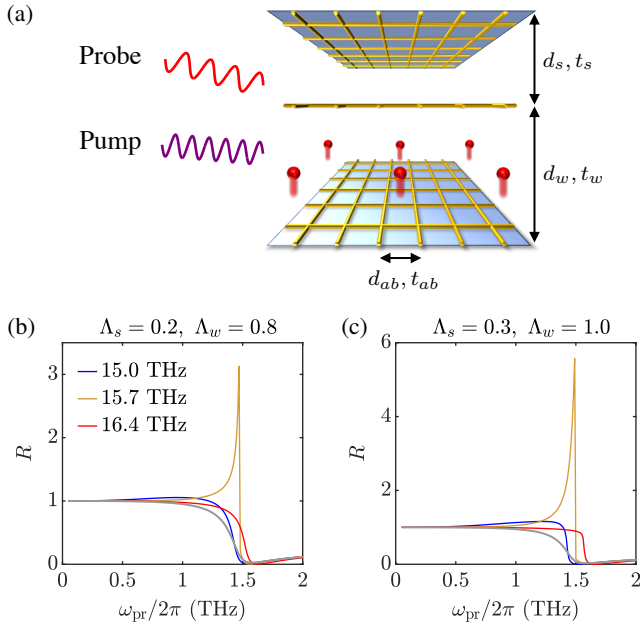


FIG. 4. Phonon mediated amplification of terahertz radiation in a bilayer cuprate. (a) Schematic illustration of the pump-probe dynamics in a bilayer cuprate. The superconducting order parameter is discretized on a layered lattice. The pump excites a phonon mode, represented by the red atoms moving along the c axis. Thus, the interlayer tunneling coefficients $t_{s,w}$ become time-dependent, which modifies the plasmonic response to the c -axis polarized probe. In (b) and (c), the reflectivity at normal incidence is shown for two choices of the modulation amplitudes of the interlayer tunneling coefficients t_s and t_w , respectively. The pump frequencies for the stronger modulation in (c) are the same as indicated for the weaker modulation in (b). Gray lines correspond to the undriven case. The probe strength is $E_{\text{pr}} = 1$ kV/cm. The lower and upper Josephson plasma frequencies are $\omega_{J1}/2\pi = 2$ THz and $\omega_{J2}/2\pi = 14.3$ THz, respectively [37].

coefficients time-dependent [42, 43], i.e.,

$$t_{s,w} \rightarrow t_{s,w} [1 \pm \Lambda_{s,w} \cos(\omega_{\text{dr}} t)]. \quad (5)$$

This captures a phononic excitation with a wavelength that is large compared to the system size of the simulation. As before, the reflectivity is calculated numerically by adding a probe to the equations of motion for the z component of the electromagnetic vector potential. We assume the existence of a suitable phonon resonance such that ω_{dr} is blue-detuned from the upper plasma frequency ω_{J2} .

In Figs. 4(b) and 4(c), we show that the phonon mediated pump has a similar effect as the plasmonic excitations discussed before. This analogy derives from tunneling terms of the form $\sim t_{k,r} A_{k,r}^2$ in the Lagrangian. That is, the parametric amplification of the terahertz probe is enabled by the cubic coupling of the tunneling coefficients and the vector potential. In contrast to the case of Higgs mode mediated amplification, the pump does

not primarily couple to the vector potential but to the tunneling coefficients, which models the excited phonon mode. Consistent with the Higgs mode mediated amplification of terahertz radiation, the maximum gain is realized when the detuning $\omega_{\text{dr}} - \omega_{J2}$ approaches the frequency of the lower reflectivity edge at $\omega_{J1}/\sqrt{2}$. However, the modified pump protocol and the bilayer structure alter the results in two aspects. Firstly, the detuning must be smaller than the lower Josephson plasma frequency ω_{J1} to achieve a reflectivity $R > 1$. Secondly, the reflectivity edge is slightly red-shifted for the phonon mediated pump, while it is slightly blue-shifted in the presence of the plasmonic excitations. The amplification of terahertz radiation is feasible up to probe strengths of ~ 100 kV/cm [37]. Note that the amplification mechanism also works if the frequency of the excited phonon mode is slightly blue-detuned from the lower plasma frequency. However, this requires a pump frequency of the order of 1 THz [44], which is in the frequency range that lacks suitable radiation sources.

Finally, we investigate the phonon mediated amplification of terahertz signals at nonzero temperature T . To obtain the c -axis conductivity $\sigma(\omega_{\text{pr}})$, we simulate an ensemble of several hundred trajectories for a bilayer system of $40 \times 40 \times 4$ sites. We evaluate the ratio of the sample averages of $J_z(\omega_{\text{pr}})$ and $E_z(\omega_{\text{pr}})$ for each trajectory before taking the ensemble average. We then calculate the reflectivity $R(\omega_{\text{pr}})$ using Eq. (4). As shown in Fig. 5, the phonon mediated amplification of terahertz radiation is effective at $\sim 20\%$ of T_c despite the thermal broadening of the parametric resonance expected at $\omega_{\text{pr}}/2\pi \approx 1$ THz. Importantly, the real part of the conductivity is negative at frequencies around 1 THz and below, leading to a reflectivity $R > 1$ in this regime. Additionally, we observe

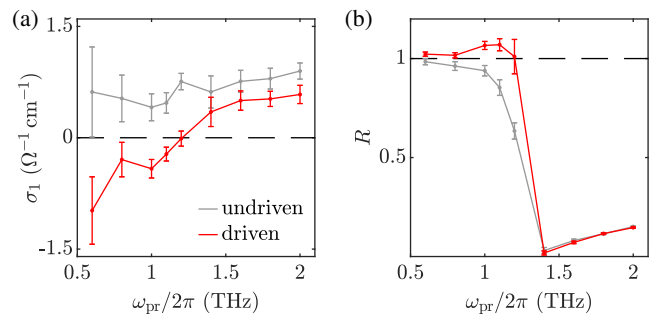


FIG. 5. Phonon mediated amplification of terahertz radiation in a bilayer cuprate at $T = 5$ K $\sim 0.2T_c$. (a) Real part of the optical conductivity. (b) Reflectivity at normal incidence. The pump frequency is $\omega_{\text{dr}}/2\pi = 14.8$ THz, and the modulation amplitudes are $\Lambda_s = 0.2$ and $\Lambda_w = 0.8$. The error bars indicate the standard errors of the ensemble averages. The probe strength is $E_{\text{pr}} = 30$ kV/cm. The bilayer system is the same as in Fig. 4. Note that the upper Josephson plasma frequency is shifted to $\omega_{J2} \approx 13.8$ THz due to thermal fluctuations.

a parametric enhancement of the imaginary part of the low-frequency conductivity at zero and nonzero temperature [37], see also [19, 42, 43, 45].

In conclusion, we propose a terahertz amplification technology based on parametric amplification in high- T_c superconductors, utilizing an optical pump mechanism. A key feature of the amplifier and its underlying mechanism is that the enhancement of the reflectivity is controlled via the pump frequency and the pump strength. Furthermore, the operation of the amplifier is not limited to pulsed pump operation but can be operated continuously in principle. Superconductors are promising candidates to induce a reflectivity $R > 1$ because their low-frequency reflectivity is close to 1 in equilibrium. We emphasize, however, that the mechanism we put forth can not only be realized in cuprate superconductors but also in other materials with collective modes that couple nonlinearly to light. The parametric amplification of terahertz signals is limited by the finite penetration depth of the pump, which is typically smaller than the penetration depth of the probe [17, 46, 47]. To reduce the mismatch of the penetration depths of the pump and the probe, we propose to choose a large incident angle for the probe beam while orienting the pump beam parallel to the surface normal, see Fig. 1.

Our proposed terahertz amplifier advances pump-probe experiments on high- T_c superconductors towards a realistic technology. It motivates a demonstration of a stable and sufficiently strong enhancement of the reflectivity above 1 and the design of an optical cavity as shown in Fig. 1, with the purpose of developing coherent radiation sources in the terahertz regime.

We thank Reinhold Kleiner, Lukas Broers, and Jim Skulte for stimulating discussions. This work is supported by the Deutsche Forschungsgemeinschaft (DFG) in the framework of SFB 925, Project No. 170620586, and the Cluster of Excellence ‘‘Advanced Imaging of Matter’’ (EXC 2056), Project No. 390715994.

[1] B. Ferguson and X. C. Zhang, Materials for terahertz science and technology, *Nat. Mater.* **1**, 26 (2002).
 [2] M. Tonouchi, Cutting-edge terahertz technology, *Nat. Photonics* **1**, 97 (2007).
 [3] E. Pickwell and V. P. Wallace, Biomedical applications of terahertz technology, *J. Phys. D: Appl. Phys.* **39**, R301 (2006).
 [4] H. Y. Hwang, S. Fleischer, N. C. Brandt, B. G. P. Jr., M. Liu, K. Fan, A. Sternbach, X. Zhang, R. D. Averitt, and K. A. Nelson, A review of non-linear terahertz spectroscopy with ultrashort tabletop-laser pulses, *J. Mod. Opt.* **62**, 1447 (2015).
 [5] D. M. Mittleman, Twenty years of terahertz imaging, *Opt. Express* **26**, 9417 (2018).
 [6] B. S. Williams, Terahertz quantum-cascade lasers, *Nat. Photonics* **1**, 517 (2007).

[7] S. Kumar, Recent progress in terahertz quantum cascade lasers, *IEEE J. Sel. Top. Quantum Electron.* **17**, 38 (2011).
 [8] M. Asada, S. Suzuki, and N. Kishimoto, Resonant tunneling diodes for sub-terahertz and terahertz oscillators, *Jpn. J. Appl. Phys.* **47**, 4375 (2008).
 [9] M. Feiginov, H. Kanaya, S. Suzuki, and M. Asada, Operation of resonant-tunneling diodes with strong back injection from the collector at frequencies up to 1.46 THz, *Appl. Phys. Lett.* **104**, 243509 (2014).
 [10] U. Welp, K. Kadowaki, and R. Kleiner, Superconducting emitters of THz radiation, *Nat. Photonics* **7**, 702 (2013).
 [11] R. Kleiner and H. Wang, Terahertz emission from $\text{Bi}_2\text{Sr}_2\text{CaCu}_2\text{O}_{8+x}$ intrinsic Josephson junction stacks, *J. Appl. Phys.* **126**, 171101 (2019).
 [12] R. Cattaneo, E. A. Borodianskyi, A. A. Kalenyuk, and V. M. Krasnov, Superconducting THz sources with 12% power efficiency, arXiv e-prints (2021), [arXiv:2109.00976 \[cond-mat.supr-con\]](https://arxiv.org/abs/2109.00976).
 [13] J. A. Giordmaine and R. C. Miller, Tunable coherent parametric oscillation in LiNbO_3 at optical frequencies, *Phys. Rev. Lett.* **14**, 973 (1965).
 [14] S. A. Akhmanov, A. I. Kovrigin, A. S. Piskarskas, V. V. Fadeev, and R. V. Khokhlov, Observation of parametric amplification in the optical range, *JETP Lett.* **2**, 191 (1965).
 [15] F. Duarte, *Tunable Laser Applications*, 3rd ed. (CRC Press, Boca Raton, 2016).
 [16] G. Chiriacò, A. J. Millis, and I. L. Aleiner, Transient superconductivity without superconductivity, *Phys. Rev. B* **98**, 220510 (2018).
 [17] M. Buzzi, G. Jotzu, A. Cavalleri, J. I. Cirac, E. A. Demler, B. I. Halperin, M. D. Lukin, T. Shi, Y. Wang, and D. Podolsky, Higgs-mediated optical amplification in a nonequilibrium superconductor, *Phys. Rev. X* **11**, 011055 (2021).
 [18] G. Homann, J. G. Cosme, and L. Mathey, Higgs time crystal in a high- T_c superconductor, *Phys. Rev. Research* **2**, 043214 (2020).
 [19] G. Homann, J. G. Cosme, J. Okamoto, and L. Mathey, Higgs mode mediated enhancement of interlayer transport in high- T_c cuprate superconductors, *Phys. Rev. B* **103**, 224503 (2021).
 [20] L. Broers and L. Mathey, Observing light-induced Floquet band gaps in the longitudinal conductivity of graphene (2021), [arXiv:2103.01949 \[cond-mat.mes-hall\]](https://arxiv.org/abs/2103.01949).
 [21] T. Koyama and M. Tachiki, I - V characteristics of Josephson-coupled layered superconductors with longitudinal plasma excitations, *Phys. Rev. B* **54**, 16183 (1996).
 [22] D. van der Marel and A. A. Tsvetkov, Transverse-optical Josephson plasmons: Equations of motion, *Phys. Rev. B* **64**, 024530 (2001).
 [23] T. Koyama, Josephson plasma resonances and optical properties in high- T_c superconductors with alternating junction parameters, *J. Phys. Soc. Jpn.* **71**, 2986 (2002).
 [24] D. Dulić, A. Pimenov, D. van der Marel, D. M. Broun, S. Kamal, W. N. Hardy, A. A. Tsvetkov, I. M. Sutjaha, R. Liang, A. A. Menovsky, A. Loidl, and S. S. Saxena, Observation of the transverse optical plasmon in $\text{SmLa}_{0.8}\text{Sr}_{0.2}\text{CuO}_{4-\delta}$, *Phys. Rev. Lett.* **86**, 4144 (2001).
 [25] H. Shibata and T. Yamada, Double Josephson plasma resonance in T^* phase $\text{SmLa}_{1-x}\text{Sr}_x\text{CuO}_{4-\delta}$, *Phys. Rev. Lett.* **81**, 3519 (1998).

- [26] R. Matsunaga, N. Tsuji, H. Fujita, A. Sugioka, K. Makise, Y. Uzawa, H. Terai, Z. Wang, H. Aoki, and R. Shimano, Light-induced collective pseudospin precession resonating with Higgs mode in a superconductor, *Science* **345**, 1145 (2014).
- [27] N. Tsuji and H. Aoki, Theory of Anderson pseudospin resonance with Higgs mode in superconductors, *Phys. Rev. B* **92**, 064508 (2015).
- [28] K. Katsumi, N. Tsuji, Y. I. Hamada, R. Matsunaga, J. Schneeloch, R. D. Zhong, G. D. Gu, H. Aoki, Y. Gallais, and R. Shimano, Higgs mode in the d -wave superconductor $\text{Bi}_2\text{Sr}_2\text{CaCu}_2\text{O}_{8+x}$ driven by an intense terahertz pulse, *Phys. Rev. Lett.* **120**, 117001 (2018).
- [29] H. Chu, M.-J. Kim, K. Katsumi, S. Kovalev, R. D. Dawson, L. Schwarz, N. Yoshikawa, G. Kim, D. Putzky, Z. Z. Li, H. Raffy, S. Germanskiy, J.-C. Deinert, N. Awari, I. Ilyakov, B. Green, M. Chen, M. Bawatna, G. Christiani, G. Logvenov, Y. Gallais, A. V. Boris, B. Keimer, A. P. Schnyder, D. Manske, M. Gensch, Z. Wang, R. Shimano, and S. Kaiser, Phase-resolved Higgs response in superconducting cuprates, *Nat. Commun.* **11**, 1793 (2020).
- [30] R. Shimano and N. Tsuji, Higgs mode in superconductors, *Annu. Rev. Condens. Matter Phys.* **11**, 103 (2020).
- [31] L. Schwarz and D. Manske, Theory of driven Higgs oscillations and third-harmonic generation in unconventional superconductors, *Phys. Rev. B* **101**, 184519 (2020).
- [32] G. Seibold, M. Udina, C. Castellani, and L. Benfatto, Third harmonic generation from collective modes in disordered superconductors, *Phys. Rev. B* **103**, 014512 (2021).
- [33] C. M. Varma, Higgs boson in superconductors, *J. Low Temp. Phys.* **126**, 901 (2002).
- [34] D. Pekker and C. Varma, Amplitude/Higgs modes in condensed matter physics, *Annu. Rev. Condens. Matter Phys.* **6**, 269 (2015).
- [35] M. Machida and T. Koyama, Localized rotating-modes in capacitively coupled intrinsic Josephson junctions: Systematic study of branching structure and collective dynamical instability, *Phys. Rev. B* **70**, 024523 (2004).
- [36] B. Josephson, Possible new effects in superconductive tunnelling, *Phys. Lett.* **1**, 251 (1962).
- [37] See Supplemental Material for an analytical estimate of Higgs mode mediated amplification of terahertz radiation in monolayer cuprates, details of the three-dimensional lattice gauge model, simulation parameters of the bilayer cuprate, information on the thermal phase transition, dependence of the reflectivity on the probe strength, and parametric enhancement of interlayer transport.
- [38] F. Peronaci, M. Schiró, and M. Capone, Transient dynamics of d -wave superconductors after a sudden excitation, *Phys. Rev. Lett.* **115**, 257001 (2015).
- [39] R. Mankowsky, A. Subedi, M. Först, S. O. Mariager, M. Chollet, H. T. Lemke, J. S. Robinson, J. M. Glowina, M. P. Minitti, A. Frano, M. Fechner, N. A. Spaldin, T. Loew, B. Keimer, A. Georges, and A. Cavalleri, Non-linear lattice dynamics as a basis for enhanced superconductivity in $\text{YBa}_2\text{Cu}_3\text{O}_{6.5}$, *Nature* **516**, 71 (2014).
- [40] R. Mankowsky, M. Först, T. Loew, J. Porras, B. Keimer, and A. Cavalleri, Coherent modulation of the $\text{YBa}_2\text{Cu}_3\text{O}_{6+x}$ atomic structure by dispersive stimulated ionic raman scattering, *Phys. Rev. B* **91**, 094308 (2015).
- [41] V. L. Ginzburg and L. D. Landau, On the theory of superconductivity, *Zh. Eksp. Teor. Fiz.* **20**, 1064 (1950).
- [42] J.-i. Okamoto, A. Cavalleri, and L. Mathey, Theory of enhanced interlayer tunneling in optically driven high- T_c superconductors, *Phys. Rev. Lett.* **117**, 227001 (2016).
- [43] J.-i. Okamoto, W. Hu, A. Cavalleri, and L. Mathey, Transiently enhanced interlayer tunneling in optically driven high- T_c superconductors, *Phys. Rev. B* **96**, 144505 (2017).
- [44] D. N. Basov and T. Timusk, Electrodynamics of high- T_c superconductors, *Rev. Mod. Phys.* **77**, 721 (2005).
- [45] S. J. Denny, S. R. Clark, Y. Laplace, A. Cavalleri, and D. Jaksch, Proposed parametric cooling of bilayer cuprate superconductors by terahertz excitation, *Phys. Rev. Lett.* **114**, 137001 (2015).
- [46] W. Hu, S. Kaiser, D. Nicoletti, C. R. Hunt, I. Gierz, M. C. Hoffmann, M. Le Tacon, T. Loew, B. Keimer, and A. Cavalleri, Optically enhanced coherent transport in $\text{YBa}_2\text{Cu}_3\text{O}_{6.5}$ by ultrafast redistribution of interlayer coupling, *Nat. Mater.* **13**, 705 (2014).
- [47] S. Kaiser, C. R. Hunt, D. Nicoletti, W. Hu, I. Gierz, H. Y. Liu, M. Le Tacon, T. Loew, D. Haug, B. Keimer, and A. Cavalleri, Optically induced coherent transport far above T_c in underdoped $\text{YBa}_2\text{Cu}_3\text{O}_{6+\delta}$, *Phys. Rev. B* **89**, 184516 (2014).

Supplemental Material for Terahertz amplifiers based on gain reflectivity in cuprate superconductors

Guido Homann,¹ Jayson G. Cosme,² and Ludwig Mathey^{1,3}

¹*Zentrum für Optische Quantentechnologien and Institut für Laserphysik, Universität Hamburg, 22761 Hamburg, Germany*

²*National Institute of Physics, University of the Philippines, Diliman, Quezon City 1101, Philippines*

³*The Hamburg Centre for Ultrafast Imaging, Luruper Chaussee 149, 22761 Hamburg, Germany*

CONTENTS

I. Analytical estimate of Higgs mode mediated amplification of terahertz radiation in monolayer cuprates	2
II. Three-dimensional lattice gauge model	4
III. Simulation parameters of the bilayer cuprate	5
IV. Thermal phase transition	6
V. Dependence of the reflectivity on the probe strength	7
VI. Parametric enhancement of interlayer transport	8
References	8

I. ANALYTICAL ESTIMATE OF HIGGS MODE MEDIATED AMPLIFICATION OF TERAHERTZ RADIATION IN MONOLAYER CUPRATES

Here, we consider a monolayer cuprate superconductor at zero temperature. Since the system is driven by a c -axis polarized electric field, it exhibits no in-plane dynamics. Additionally, we employ periodic boundary conditions so that the cuprate can be described by the two following equations of motion,

$$\ddot{\theta} + \gamma_J \dot{\theta} + \omega_J^2 \sin(\theta)(1+h)^2 = j, \quad (1)$$

$$\ddot{h} + \gamma_H \dot{h} + \omega_H^2 \left(h + \frac{3}{2}h^2 + \frac{1}{2}h^3 \right) + 2\alpha\omega_J^2 [1 - \cos(\theta)](1+h) = 0. \quad (2)$$

Neglecting all nonlinear terms except for the quadratic coupling between the Higgs mode h and the plasma mode θ , we find

$$\ddot{\theta} + \gamma_J \dot{\theta} + \omega_J^2 \theta + 2\omega_J^2 \theta h = j, \quad (3)$$

$$\ddot{h} + \gamma_H \dot{h} + \omega_H^2 h + \alpha\omega_J^2 \theta^2 = 0, \quad (4)$$

as in Refs. [1, 2]. Now, we expand j , θ , and h in the form

$$f = f^{(0)} + \lambda f^{(1)} + \lambda^2 f^{(2)} + \lambda^3 f^{(3)} + \mathcal{O}(\lambda^4), \quad (5)$$

where $\lambda \ll 1$ is a small expansion parameter. We take the current j induced by the pump and the probe as

$$j^{(1)} = j_{\text{dr},1} e^{-i\omega_{\text{dr}} t} + j_{\text{pr},1} e^{-i\omega_{\text{pr}} t} + \text{c.c.} \quad (6)$$

Hence, there are no zeroth order contributions and we obtain

$$\theta^{(1)} = \theta_{\text{dr},1} e^{-i\omega_{\text{dr}} t} + \theta_{\text{pr},1} e^{-i\omega_{\text{pr}} t} + \text{c.c.}, \quad (7)$$

$$h^{(1)} = 0 \quad (8)$$

in first order, where

$$\theta_{\text{dr},1} = \frac{j_{\text{dr},1}}{\omega_J^2 - \omega_{\text{dr}}^2 - i\gamma_J \omega_{\text{dr}}}, \quad (9)$$

$$\theta_{\text{pr},1} = \frac{j_{\text{pr},1}}{\omega_J^2 - \omega_{\text{pr}}^2 - i\gamma_J \omega_{\text{pr}}}. \quad (10)$$

In second order, we have

$$\theta^{(2)} = 0, \quad (11)$$

$$h^{(2)} = h_0 + h_1 e^{-2i\omega_{\text{dr}} t} + h_2 e^{-2i\omega_{\text{pr}} t} + h_3 e^{-i(\omega_{\text{dr}} - \omega_{\text{pr}}) t} + h_4 e^{-i(\omega_{\text{dr}} + \omega_{\text{pr}}) t} + \text{c.c.}, \quad (12)$$

where

$$h_0 = -\frac{2\alpha\omega_J^2}{\omega_H^2} (|\theta_{\text{dr},1}|^2 + |\theta_{\text{pr},1}|^2), \quad (13)$$

$$h_1 = \frac{\alpha\omega_J^2 \theta_{\text{dr},1}^2}{4\omega_{\text{dr}}^2 - \omega_H^2 + 2i\gamma_H \omega_{\text{dr}}}, \quad (14)$$

$$h_2 = \frac{\alpha\omega_J^2 \theta_{\text{pr},1}^2}{4\omega_{\text{pr}}^2 - \omega_H^2 + 2i\gamma_H \omega_{\text{pr}}}, \quad (15)$$

$$h_3 = \frac{2\alpha\omega_J^2 \theta_{\text{dr},1} \theta_{\text{pr},1}^*}{(\omega_{\text{dr}} - \omega_{\text{pr}})^2 - \omega_H^2 + i\gamma_H (\omega_{\text{dr}} - \omega_{\text{pr}})}, \quad (16)$$

$$h_4 = \frac{2\alpha\omega_J^2 \theta_{\text{dr},1} \theta_{\text{pr},1}}{(\omega_{\text{dr}} + \omega_{\text{pr}})^2 - \omega_H^2 + i\gamma_H (\omega_{\text{dr}} + \omega_{\text{pr}})}. \quad (17)$$

In third order, we find the following correction for the vector potential at the probe frequency,

$$\theta_{\text{pr},3} = \frac{2\omega_J^2 (h_0 \theta_{\text{pr},1} + h_2 \theta_{\text{pr},1}^* + h_3 \theta_{\text{dr},1} + h_4 \theta_{\text{dr},1}^*)}{\omega_{\text{pr}}^2 - \omega_J^2 + i\gamma_J \omega_{\text{pr}}}. \quad (18)$$

We consider a probe with $|j_{\text{pr},1}| \ll |j_{\text{dr},1}|$ and $\omega_{\text{pr}} = \omega_{\text{dr}} - \omega_{\text{H}}$ such that we can neglect the h_2 term. Moreover, we assume near-resonant driving, i.e., $\omega_{\text{dr}} \simeq \omega_{\text{H}}$, to simplify the denominators in Eqs. (16) and (17),

$$\begin{aligned} \theta_{\text{pr},3} &\approx \frac{-4\alpha\omega_{\text{J}}^4|\theta_{\text{dr},1}|^2\theta_{\text{pr},1}}{\omega_{\text{pr}}^2 - \omega_{\text{J}}^2 + i\gamma_{\text{J}}\omega_{\text{pr}}}\left(\frac{1}{\omega_{\text{H}}^2} + \frac{2}{i\gamma_{\text{H}}\omega_{\text{H}}}\right) \\ &\approx \frac{4\alpha\omega_{\text{J}}^4|j_{\text{dr},1}|^2j_{\text{pr},1}(\gamma_{\text{H}} - 2i\omega_{\text{H}})}{\gamma_{\text{H}}\omega_{\text{H}}^2[(\omega_{\text{dr}} - \omega_{\text{H}})^2 - \omega_{\text{J}}^2 + i\gamma_{\text{J}}(\omega_{\text{dr}} - \omega_{\text{H}})]^2[(\omega_{\text{dr}}^2 - \omega_{\text{J}}^2)^2 + \gamma_{\text{J}}^2\omega_{\text{dr}}^2]}. \end{aligned} \quad (19)$$

As $\dot{\theta} = 2edE/\hbar$ [3], the optical conductivity is given by

$$\sigma(\omega_{\text{pr}}) = \frac{i\epsilon_z\epsilon_0j(\omega_{\text{pr}})}{\omega_{\text{pr}}\theta(\omega_{\text{pr}})} = \frac{i\epsilon_z\epsilon_0\lambda j_{\text{pr},1}}{\omega_{\text{pr}}(\lambda\theta_{\text{pr},1} + \lambda^3\theta_{\text{pr},3})}, \quad (20)$$

and we obtain

$$\begin{aligned} \sigma(\omega_{\text{pr}} = \omega_{\text{dr}} - \omega_{\text{H}}) &\approx \frac{-i\epsilon_z\epsilon_0\gamma_{\text{H}}\omega_{\text{H}}^2[(\omega_{\text{dr}} - \omega_{\text{H}})^2 - \omega_{\text{J}}^2 + i\gamma_{\text{J}}(\omega_{\text{dr}} - \omega_{\text{H}})]^2[(\omega_{\text{dr}}^2 - \omega_{\text{J}}^2)^2 + \gamma_{\text{J}}^2\omega_{\text{dr}}^2](\omega_{\text{dr}} - \omega_{\text{H}})^{-1}}{\gamma_{\text{H}}\omega_{\text{H}}^2[(\omega_{\text{dr}} - \omega_{\text{H}})^2 - \omega_{\text{J}}^2 + i\gamma_{\text{J}}(\omega_{\text{dr}} - \omega_{\text{H}})][(\omega_{\text{dr}}^2 - \omega_{\text{J}}^2)^2 + \gamma_{\text{J}}^2\omega_{\text{dr}}^2] - 4\alpha\omega_{\text{J}}^4|j_{\text{dr}}|^2(\gamma_{\text{H}} - 2i\omega_{\text{H}})}, \end{aligned} \quad (21)$$

with the original pump amplitude $j_{\text{dr}} = \lambda j_{\text{dr},1}$. Taking $j_{\text{dr}} = 0$ leads to the equilibrium solution

$$\sigma_1(\omega_{\text{pr}} = \omega_{\text{dr}} - \omega_{\text{H}}) \approx \epsilon_z\epsilon_0\gamma_{\text{J}}. \quad (22)$$

for the real part of the conductivity. In the above calculation, ω_{pr} is formally negative for $\omega_{\text{dr}} < \omega_{\text{H}}$. However, our analytical prediction has the property that $\sigma_1(\omega_{\text{pr}}) = \sigma_1(-\omega_{\text{pr}})$, as characteristic for Fourier transforms of real quantities. In Fig. 1, the real part of the conductivity at $\omega_{\text{pr}} = \omega_{\text{dr}} - \omega_{\text{H}}$ is displayed as a function of the pump frequency according to our analytical estimate in Eq. (21). The field strength E_0 of the applied electric field gives rise to the pump amplitude $|j_{\text{dr}}| = ed\omega_{\text{dr}}E_0/\hbar\epsilon_r$. Consistent with the results shown in the main text, we find a negative conductivity when the pump frequency is slightly blue-detuned from the Higgs frequency. On the other hand, the conductivity is positive for red-detuned pump frequencies. A quantitative comparison to the numerical results reveals notable deviations, which are due to the approximations made in the derivation of Eq. (21).

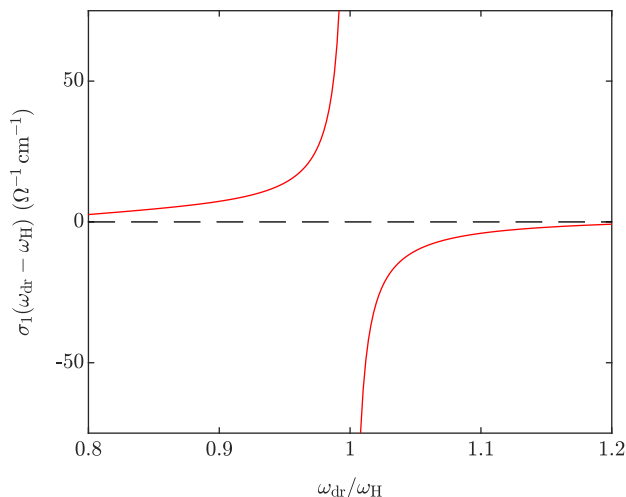


FIG. 1. Analytical estimate of the optical conductivity of a monolayer cuprate, in which Josephson plasma oscillations are optically driven. The negative conductivity for $\omega_{\text{dr}} \gtrsim \omega_{\text{H}}$ indicates the Higgs mode mediated amplification of terahertz radiation. As in Fig. 2 in the main text, the Josephson plasma frequency is $\omega_{\text{J}}/2\pi = 2$ THz and the Higgs frequency is $\omega_{\text{H}}/2\pi = 6$ THz. The remaining parameters are $E_0 = 300$ kV/cm, $\gamma_{\text{J}}/2\pi = 0.5$ THz, $\gamma_{\text{H}}/2\pi = 1$ THz, $\alpha = 1$, $\epsilon_r = 4$, and $d = 10$ Å.

II. THREE-DIMENSIONAL LATTICE GAUGE MODEL

In this section, we present the lattice gauge model [1, 2] used for the simulations of phonon mediated amplification of terahertz radiation in a bilayer cuprate. As mentioned in the main text, the static part of the Lagrangian is a discretized version of the Ginzburg-Landau free energy [4]. While the order parameter $\psi_{\mathbf{r}}(t)$ is located on the lattice sites, each component of the electromagnetic vector potential $A_{k,\mathbf{r}}(t)$ is defined on the bond between the site \mathbf{r} and its nearest neighbor in the k direction. Intrinsic Josephson junctions between neighboring lattice sites enable Cooper pairs to move through the sample. To model a bilayer structure, we introduce two types of junctions along the c axis, strong junctions corresponding to intrabilayer tunneling and weak junctions corresponding to interbilayer tunneling. We assign the strong (weak) junctions to the even (odd) layers. The strong junctions have a spacing d_s and a tunneling coefficient t_s , and the weak junctions have a spacing d_w and a tunneling coefficient t_w . The in-plane junctions are characterized by the discretization length d_{ab} and the tunneling coefficient $t_{ab} \gg t_s \gg t_w$. Note that we suppose the z direction to be aligned with the c axis of the crystal.

The Lagrangian of the lattice gauge model is

$$\mathcal{L} = \mathcal{L}_{\text{sc}} + \mathcal{L}_{\text{em}} + \mathcal{L}_{\text{kin}}. \quad (23)$$

The first term is the $|\psi|^4$ model of the superconducting condensate in the absence of Cooper pair tunneling,

$$\mathcal{L}_{\text{sc}} = \sum_{\mathbf{r}} K \hbar^2 |\partial_t \psi_{\mathbf{r}}|^2 + \mu |\psi_{\mathbf{r}}|^2 - \frac{g}{2} |\psi_{\mathbf{r}}|^4, \quad (24)$$

with the fixed Ginzburg-Landau coefficients μ and g . The coefficient K describes the magnitude of the dynamical term [5, 6].

The electromagnetic part \mathcal{L}_{em} accounts for the Coulomb interaction between the Cooper pairs and the screening due to bound charges in the material,

$$\mathcal{L}_{\text{em}} = \sum_{k,\mathbf{r}} \frac{\kappa_{k,\mathbf{r}} \epsilon_{k,\mathbf{r}} \epsilon_0}{2} E_{k,\mathbf{r}}^2 - \frac{\kappa_{z,\mathbf{r}}}{\kappa_{k,\mathbf{r}} \beta_{k,\mathbf{r}}^2 \mu_0} \left[1 - \cos(\beta_{k,\mathbf{r}} B_{k,\mathbf{r}}) \right], \quad (25)$$

where $E_{k,\mathbf{r}}$ denotes the k -component of the electric field. Note that we choose the temporal gauge for our calculations, i.e., $E_{k,\mathbf{r}} = -\partial_t A_{k,\mathbf{r}}$. The magnetic field components $B_{k,\mathbf{r}} = \epsilon_{klm} \delta_l A_{m,\mathbf{r}}$ are centered about the plaquettes of the lattice. We calculate the spatial derivatives according to $\delta_l A_{m,\mathbf{r}} = (A_{m,\mathbf{r}'(l)} - A_{m,\mathbf{r}})/d_{l,\mathbf{r}}$, where $\mathbf{r}'(l)$ is the neighboring site of \mathbf{r} in the l direction. The length of the bond $d_{l,\mathbf{r}}$ is d_{ab} for in-plane junctions, d_s for strong junctions, and d_w for weak junctions. The dielectric permittivities are $\epsilon_{x,\mathbf{r}} = \epsilon_{y,\mathbf{r}} = \epsilon_{ab}$ for in-plane junctions, $\epsilon_{z,\mathbf{r}} = \epsilon_s$ for strong junctions, and $\epsilon_{z,\mathbf{r}} = \epsilon_w$ for weak junctions. The other prefactors in Eq. (25) account for the anisotropic lattice geometry. Introducing $d_c = (d_s + d_w)/2$, one can write $\kappa_{x,\mathbf{r}} = \kappa_{y,\mathbf{r}} = 1$ and $\kappa_{z,\mathbf{r}} = d_{z,\mathbf{r}}/d_c$, while $\beta_{x,\mathbf{r}} = \beta_{y,\mathbf{r}} = 2ed_{ab}d_{z,\mathbf{r}}/\hbar$ and $\beta_{z,\mathbf{r}} = 2ed_{ab}^2/\hbar$.

The kinetic part of the Lagrangian is given by

$$\mathcal{L}_{\text{kin}} = - \sum_{k,\mathbf{r}} t_{k,\mathbf{r}} |\psi_{\mathbf{r}'(k)} - \psi_{\mathbf{r}} e^{ia_{k,\mathbf{r}}}|^2. \quad (26)$$

The unitless vector potential $a_{k,\mathbf{r}} = -2ed_{k,\mathbf{r}}A_{k,\mathbf{r}}/\hbar$ directly couples to the phase of the superconducting field. Thus, it does not only ensure the local gauge-invariance of \mathcal{L}_{kin} , but it also gives rise to a nonlinear coupling between the Higgs mode and the electromagnetic field. The Lagrangian (23) is particle-hole symmetric due to its invariance under $\psi_{\mathbf{r}} \rightarrow \psi_{\mathbf{r}}^*$.

Including damping terms and thermal fluctuations, the equations of motion read

$$\partial_t^2 \psi_{\mathbf{r}} = \frac{1}{K \hbar^2} \frac{\partial \mathcal{L}}{\partial \psi_{\mathbf{r}}^*} - \gamma_{\text{H}} \partial_t \psi_{\mathbf{r}} + \xi_{\mathbf{r}}, \quad (27)$$

$$\partial_t^2 A_{x,\mathbf{r}} = \frac{1}{\epsilon_{ab} \epsilon_0} \frac{\partial \mathcal{L}}{\partial A_{x,\mathbf{r}}} - \gamma_{ab} \partial_t A_{x,\mathbf{r}} + \eta_{x,\mathbf{r}}, \quad (28)$$

$$\partial_t^2 A_{y,\mathbf{r}} = \frac{1}{\epsilon_{ab} \epsilon_0} \frac{\partial \mathcal{L}}{\partial A_{y,\mathbf{r}}} - \gamma_{ab} \partial_t A_{y,\mathbf{r}} + \eta_{y,\mathbf{r}}, \quad (29)$$

$$\partial_t^2 A_{z,\mathbf{r}} = \frac{1}{\kappa_{z,\mathbf{r}} \epsilon_{z,\mathbf{r}} \epsilon_0} \frac{\partial \mathcal{L}}{\partial A_{z,\mathbf{r}}} - \gamma_{z,\mathbf{r}} \partial_t A_{z,\mathbf{r}} + \eta_{z,\mathbf{r}}, \quad (30)$$

where $\xi_{\mathbf{r}}$ and $\boldsymbol{\eta}_{\mathbf{r}}$ represent the thermal fluctuations of the superconducting order parameter and the vector potential, respectively. These Langevin noise terms have a white Gaussian distribution with zero mean. The damping coefficients of the intra- and interbilayer electric fields are γ_s and γ_w , respectively. To satisfy the fluctuation-dissipation theorem, we take the noise of the order parameter as

$$\langle \text{Re}\{\xi_{\mathbf{r}}(t)\}\text{Re}\{\xi_{\mathbf{r}'}(t')\} \rangle = \frac{\gamma_{\text{H}}k_{\text{B}}T}{K\hbar^2V_0}\delta_{\mathbf{r}\mathbf{r}'}\delta(t-t'), \quad (31)$$

$$\langle \text{Im}\{\xi_{\mathbf{r}}(t)\}\text{Im}\{\xi_{\mathbf{r}'}(t')\} \rangle = \frac{\gamma_{\text{H}}k_{\text{B}}T}{K\hbar^2V_0}\delta_{\mathbf{r}\mathbf{r}'}\delta(t-t'), \quad (32)$$

$$\langle \text{Re}\{\xi_{\mathbf{r}}(t)\}\text{Im}\{\xi_{\mathbf{r}'}(t')\} \rangle = 0, \quad (33)$$

where $V_0 = d_{ab}^2d_c$. The noise correlations for the vector potential are

$$\langle \eta_{x,\mathbf{r}}(t)\eta_{x,\mathbf{r}'}(t') \rangle = \frac{2\gamma_{ab}k_{\text{B}}T}{\epsilon_{ab}\epsilon_0V_0}\delta_{\mathbf{r}\mathbf{r}'}\delta(t-t'), \quad (34)$$

$$\langle \eta_{y,\mathbf{r}}(t)\eta_{y,\mathbf{r}'}(t') \rangle = \frac{2\gamma_{ab}k_{\text{B}}T}{\epsilon_{ab}\epsilon_0V_0}\delta_{\mathbf{r}\mathbf{r}'}\delta(t-t'), \quad (35)$$

$$\langle \eta_{z,\mathbf{r}}(t)\eta_{z,\mathbf{r}'}(t') \rangle = \frac{2\gamma_{z,\mathbf{r}}k_{\text{B}}T}{\kappa_{z,\mathbf{r}}\epsilon_{z,\mathbf{r}}\epsilon_0V_0}\delta_{\mathbf{r}\mathbf{r}'}\delta(t-t'). \quad (36)$$

We employ periodic boundary conditions and integrate the differential equations using Heun's method with a step size $\Delta t = 1.6$ as.

III. SIMULATION PARAMETERS OF THE BILAYER CUPRATE

In this work, we simulate a bilayer cuprate with $40 \times 40 \times 4$ sites, choosing the parameters summarized in Table I. Our choice of μ and g implies an equilibrium condensate density $n_0 = \mu/g = 2 \times 10^{21} \text{ cm}^{-3}$ at $T = 0$. The bilayer system has two longitudinal c -axis plasma modes. Their eigenfrequencies are

$$\omega_{\text{J1},\text{J2}}^2 = \left(\frac{1}{2} + \alpha_s\right)\Omega_s^2 + \left(\frac{1}{2} + \alpha_w\right)\Omega_w^2 \mp \sqrt{\left[\left(\frac{1}{2} + \alpha_s\right)\Omega_s^2 - \left(\frac{1}{2} + \alpha_w\right)\Omega_w^2\right]^2 + 4\alpha_s\alpha_w\Omega_s^2\Omega_w^2}, \quad (37)$$

TABLE I. Model parameters of the simulated bilayer cuprate.

K (meV $^{-1}$)	1.9×10^{-5}
μ (meV)	6.0×10^{-3}
g (meV \AA^3)	3.0
$\gamma_{\text{H}}/2\pi$ (THz)	1.0
$\gamma_{ab}/2\pi$ (THz)	7.0
$\gamma_s/2\pi$ (THz)	1.5
$\gamma_w/2\pi$ (THz)	0.5
ϵ_{ab}	4
ϵ_s	2
ϵ_w	8
d_{ab} (\AA)	15
d_s (\AA)	4
d_s (\AA)	8
t_{ab} (meV)	5.2×10^{-1}
t_s (meV)	2.4×10^{-2}
t_s (meV)	1.7×10^{-3}

as follows from a sine-Gordon analysis [7, 8]. Here we introduced the bare plasma frequencies of the strong and weak junctions

$$\Omega_{s,w} = \sqrt{\frac{8t_{s,w}n_0e^2d_c d_{s,w}}{\hbar^2\epsilon_{s,w}\epsilon_0}}, \quad (38)$$

where $d_c = (d_s + d_w)/2$. The capacitive coupling constants are given by

$$\alpha_{s,w} = \frac{\epsilon_{s,w}\epsilon_0}{8Kn_0e^2d_c d_{s,w}}. \quad (39)$$

Besides, there is a transverse c -axis plasma mode with the eigenfrequency

$$\omega_T^2 = \frac{1 + 2\alpha_s + 2\alpha_w}{\alpha_s + \alpha_w} (\alpha_s\Omega_s^2 + \alpha_w\Omega_w^2). \quad (40)$$

We have $\alpha_s \approx 1.5$, $\alpha_w \approx 3.0$, $\omega_{J1}/2\pi \approx 2.0$ THz, $\omega_{J2}/2\pi \approx 14.3$ THz, and $\omega_T/2\pi \approx 13.2$ THz for the parameters specified in Table I. The in-plane plasma frequency amounts to $\omega_{ab}/2\pi \approx 70$ THz. The average c -axis permittivity is

$$\epsilon_r = \frac{(d_s + d_w)\epsilon_s\epsilon_w}{d_s\epsilon_w + d_w\epsilon_s} = 4. \quad (41)$$

IV. THERMAL PHASE TRANSITION

The thermal equilibrium at a given temperature is established as follows. We initialize the system in its ground state at $T = 0$ and let the dynamics evolve without external driving, influenced only by thermal fluctuations and dissipation. To characterize the phase transition, we introduce the order parameter

$$O = \frac{\left| \sum_{\mathbf{r} \in \text{odd}} \psi_{\mathbf{r}'(z)}^* \psi_{\mathbf{r}} e^{ia_{z,\mathbf{r}}} \right|}{\sum_{\mathbf{r}} |\psi_{\mathbf{r}}|^2}. \quad (42)$$

The sum in the numerator is taken over all lattice sites in the odd layers, and $\mathbf{r}'(z)$ denotes the neighboring site of \mathbf{r} in the z direction as usual. Thus, the order parameter measures the gauge-invariant phase coherence of the condensate across different bilayers. In our simulations, this quantity converges to a constant after 10 ps of free time evolution, indicating the onset of thermal equilibrium. For each trajectory, the order parameter is evaluated from the average of 200 measurements within a time interval of 2 ps. Finally, we take the ensemble average of 100 trajectories. As depicted in Fig. 2(a), the temperature dependence of the order parameter is reminiscent of a second order phase transition. Due to the finite size of the simulated system, the order parameter converges to a plateau with nonzero value for high temperatures. At $T_c \sim 25$ K, there is a distinct crossover.

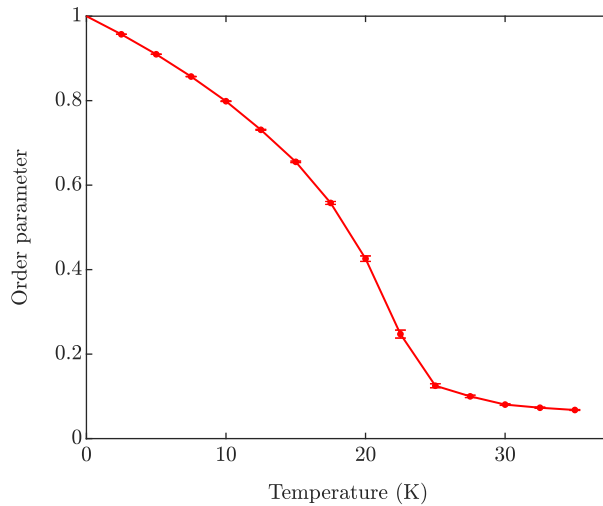


FIG. 2. Phase transition of a bilayer cuprate with $40 \times 40 \times 4$ sites and the parameters specified in Table I. The error bars indicate the standard errors of the ensemble averages.

V. DEPENDENCE OF THE REFLECTIVITY ON THE PROBE STRENGTH

Here, we investigate the dependence of the reflectivity on the probe strength. Specifically, we evaluate the reflectivity of a bilayer cuprate with oscillating interlayer tunneling coefficients t_s and t_w for various probe strengths. As one can see in Fig. 3, the results for $E_{\text{pr}} = 1$ kV/cm and $E_{\text{pr}} = 30$ kV/cm are in very good agreement. There is only a small deviation close to the maximum. This demonstrates that all the results in the main text correspond to the linear response regime. For higher probe strengths, however, the amplification peak in the reflectivity decreases and the plasma edge is shifted to lower frequencies. Remarkably, the reflectivity still exceeds 1 for probe frequencies slightly above 1 THz when the probe strength reaches 100 kV/cm.

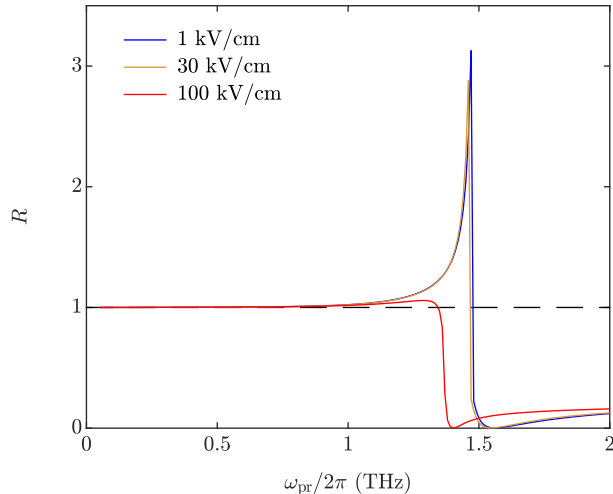


FIG. 3. Reflectivity of a bilayer cuprate in the presence of a phonon mediated pump, evaluated for various probe strengths at zero temperature. The pump frequency is $\omega_{\text{dr}}/2\pi = 15.7$ THz, and the modulation amplitudes of the interlayer tunneling coefficients are $\Lambda_s = 0.2$ and $\Lambda_w = 0.8$. See Section III for model parameters.

VI. PARAMETRIC ENHANCEMENT OF INTERLAYER TRANSPORT

In Fig. 4, we present numerical results for the imaginary part σ_2 of the c -axis optical conductivity of a bilayer cuprate, corresponding to the examples of phonon mediated amplification of terahertz radiation in Figs. 4(b) and 5 in the main text. The zero-temperature results in Fig. 4(a) show a significant enhancement of σ_2 for low probe frequencies. Our simulations at nonzero temperature indicate a qualitatively similar behavior, as visible in Fig. 4(b). A Higgs mode mediated enhancement of interlayer transport in light-driven cuprates was proposed in Ref. [2].

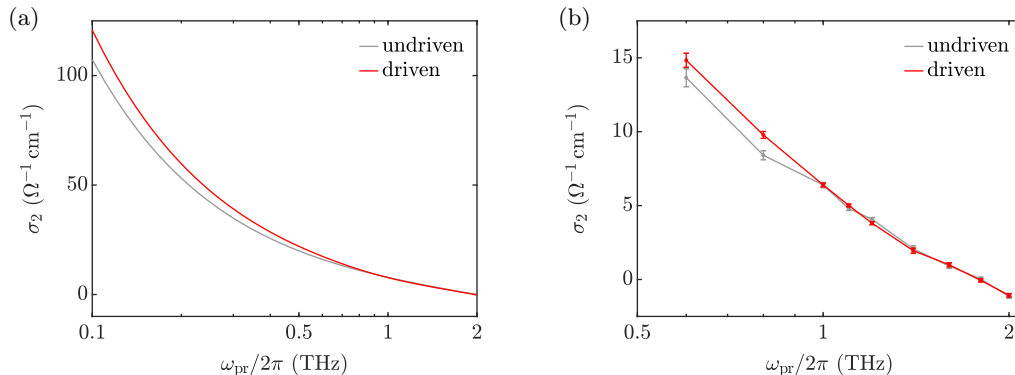


FIG. 4. Phonon mediated enhancement of interlayer transport in bilayer cuprates. (a) Imaginary part of the optical conductivity at $T = 0$. The pump frequency is $\omega_{\text{dr}}/2\pi = 15$ THz, while the upper Josephson plasma frequency is $\omega_{\text{J}2} \approx 14.3$ THz. The probe strength is $E_{\text{pr}} = 1$ kV/cm. (b) Imaginary part of the optical conductivity at $T = 5$ K $\sim 0.2T_c$. The pump frequency is $\omega_{\text{dr}}/2\pi = 14.8$ THz, while the upper Josephson plasma frequency is shifted to $\omega_{\text{J}2} \approx 13.8$ THz due to the thermal fluctuations. The probe strength is $E_{\text{pr}} = 30$ kV/cm. The error bars in (b) indicate the standard errors of the ensemble averages. In both cases, the modulation amplitudes of the interlayer tunneling coefficients are $\Lambda_s = 0.2$ and $\Lambda_w = 0.8$. See Section III for full parameter set.

-
- [1] G. Homann, J. G. Cosme, and L. Mathey, Higgs time crystal in a high- T_c superconductor, *Phys. Rev. Research* **2**, 043214 (2020).
 - [2] G. Homann, J. G. Cosme, J. Okamoto, and L. Mathey, Higgs mode mediated enhancement of interlayer transport in high- T_c cuprate superconductors, *Phys. Rev. B* **103**, 224503 (2021).
 - [3] B. Josephson, Possible new effects in superconductive tunnelling, *Phys. Lett.* **1**, 251 (1962).
 - [4] V. L. Ginzburg and L. D. Landau, On the theory of superconductivity, *Zh. Eksp. Teor. Fiz.* **20**, 1064 (1950).
 - [5] D. Pekker and C. Varma, Amplitude/Higgs modes in condensed matter physics, *Annu. Rev. Condens. Matter Phys.* **6**, 269 (2015).
 - [6] N. Tsuji and H. Aoki, Theory of Anderson pseudospin resonance with Higgs mode in superconductors, *Phys. Rev. B* **92**, 064508 (2015).
 - [7] D. van der Marel and A. A. Tsvetkov, Transverse-optical Josephson plasmons: Equations of motion, *Phys. Rev. B* **64**, 024530 (2001).
 - [8] T. Koyama, Josephson plasma resonances and optical properties in high- T_c superconductors with alternating junction parameters, *J. Phys. Soc. Jpn.* **71**, 2986 (2002).